# Detection of Co-Continuous Structures in SAN/PA6 Blends by Different Methods

*Petra Pötschke,*[1] Donald R. Paul[2]*

[1] Institut für Polymerforschung Dresden e. V., Hohe Straße 6, D - 01069 Dresden, Germany
E-mail: poe@ipfdd.de
[2] Department of Chemical Engineering and Texas Materials Institute
The University of Texas, Austin, Texas 78712, USA

**Summary**: This paper describes the 70/30 wt% composition of SAN/PA6 blends having different types of morphology, namely PA6 dispersed in SAN, a co-continuous structures of PA6 and SAN, and a "mixed structure" which exhibits PA6 particles in SAN which themselves form the matrix for smaller SAN particles. These morphologies were achieved by using different processing conditions during extrusion blending in a twin screw extruder, especially variation in the screw speed and by injection molding. Morphological analysis using SEM and TEM, solubility experiments, DMA, and oscillatory rheometry are presented. These methods were shown to be able to distinguish between the different types of morphology. In addition, DSC was used to detect the PA6 crystallization behavior.

**Keywords:** blends, differential scanning calorimetry (DSC), co-continuous structure, morphology, rheology

## Introduction

Co-continuous blends involve the coexistence of at least two continuous structures within the same volume. Blends with co-continuous structures may combine the properties of both components in a favorable way, for example mechanical moduli.

Co-continuous structures are complicated three-dimensional interpenetrating and intertwining structures that are not always isotropic. Compared to dispersed, lamellar or fibrillar structures, it is much more difficult to identify a co-continuous structure unequivocally in a melt mixed blend. Microscopic methods, like light microscopy (LM), scanning electron microscopy (SEM) or transmission electron microscopy (TEM) are often used to visualize blend structures. Microscopic methods based on thin sections which only show a cross-section of the three dimensional structure (TEM, LM) can be problematic for identifying a three dimensional co-continuous structure. Viewing of selectively etched surfaces by SEM can be more informative because it is possible to investigate, at least partially, in the third dimension. Because of the limitations of microscopic methods, indirect methods seem to be more suitable for the unequivocal identification of co-continuous structures. Extraction experiments are shown to be an easy and viable way to check for co-continuity when the components are soluble in specific

 DOI: 10.1002/masy.200350807

solvents. Measurements like dynamic mechanical analysis (DMA), stress-strain-behavior, impact properties, and melt rheology on samples with varying compositions may show a signature indicative of a co-continuous structure composition range; however, such properties generally do not provide an unequivocal indicator of structure.

The aim of the paper is to analyze different methods for their ability to distinguish between co-continuous and dispersed morphology type which were achieved at the same blend composition. Such a comparison is of interest because only then the benefits of co-continuous structures become clear. For this purpose, styrene-acrylonitrile copolymer (SAN) / polyamide 6 (PA6) blends having a composition of SAN/PA6=70/30 wt% were extruded in a twin screw extruder under different conditions, especially variation in the screw speed and by injection molding. Three different types of morphology, namely PA6 dispersed in SAN, co-continuous structures of PA6 and SAN, and a "mixed structure" which exhibits PA6 particles in SAN which themselves form the matrix for smaller SAN particles were obtained. For the comparison, morphological analysis using SEM and TEM, extraction experiments, oscillatory rheometry, and DMA were applied. In addition, DSC was used to detect the PA6 crystallization behavior.

## Materials and Methods

Blends with the composition SAN/PA6 = 70/30 wt% were made from SAN 25 (Tyril 100, Dow Chemical) and PA6 (Capron 8207F, Allied Signal). According to Kitayama et al.[1] this SAN exhibiting 25 wt% acrylonitrile has a $M_w$ value of 152,000 g/mol whereas, the PA6 has a molecular weight $M_n$ of 22,000 g/mol. According to the densities of the materials (SAN= 1.07 g/cm$^3$, polyamide = 1.13 g/cm$^3$)[1] the volume composition of the blends is SAN/PA6 = 71.1/28.9 vol%. The materials were dried under vacuum at 80°C for at least one day prior to all processing and analyzing operations. A Killion single-screw extruder (L/D=30, D= 25.4 mm) outfitted with an intensive mixing head was used to extrude the blends at 240°C with screw speeds of 40 and 80 rpm. The extrudate was drawn through an ice-water bath before being pelletized or sampled as strand. Injection molding was performed with the material extruded at 40 rpm using an Arburg Allrounder injection molding machine at 240°C to produce standard tensile bars with 3.18 mm thickness (ASTM D638 type 1).

TEM was performed on specimens cryogenically (about -20°C) microtomed perpendicular to the flow direction from the center of the strand or injection molded sample. The thin sections (thickness about 30 nm) were stained with phospotungstic acid by floating the sections on the

surface of a 2 % solution for 30 min and washed with distilled water for 20 min. By this procedure, PA6 is stained dark. TEM was carried out on a JOEL 200CX microscope operating at an acceleration voltage of 120 keV.

SEM was performed on cryofractured surfaces (along and perpendicular to the extrusion direction) and cryocut surfaces with and without etching in selective solvents. Formic acid (FA) was used to etch the PA6 phase and tetrahydrofuran (THF) to etch SAN. Investigations were done on sputtered samples using a LEO VP1530 scanning electron microscope with acceleration voltages of 6-10 kV.

Blend solubility was checked by putting one piece of about 0.1 g in 5 ml solvent at room temperature for 1 week. After that the vials were shaken and photos were taken. To dissolve PA6, formic acid (98 % Fluka) was used; to dissolve SAN, THF (99.5 % purity, Merck) was applied. Quantitative analysis was performed with 0.5 g dried blend granules in 50 ml solvent for 96 hours at room temperature. The insoluble part in THF was extracted a second time with fresh THF for 24 h. The sample extracted with formic acid was washed several days in distilled water.

Melt rheological measurements were done using a ARES oscillatory rheometer (Rheometrics Inc.) with parallel plate geometry at 240°C under nitrogen atmosphere. Frequency sweeps were performed at a strain of 5% using a highly sensitive transducer (0.02-200 g cm) on the same sample with increasing frequency from 0.1 to 100 rad/s, with decreasing frequency from 100 to 0.05 rad/s, and after that from 100 to 0.1 rad/s. The second sweep was used for the interpretation. The third sweep was performed as a control to see if changes had occurred in the material during the long annealing time in the melt, which was about 8 min for the first and the third sweep, but about 70 min for the second sweep. The sweeps showed good agreement and all torque values were found to be in the working range of the transducer (> 0.08 g cm). Strain sweeps were performed to prove that the applied strain was within the linear-viscoelastic deformation range.

Dynamical mechanical analysis was performed with the same equipment under torsion rectangular conditions on strands (PA6, SAN, extruded blends) and on the injection molded sample. A heating rate of 5 K/min and a strain of 0.05 % were applied in the temperature range of -100°C to 170°C.

Differential scanning calorimetry was performed using a DSC 7 (Perkin-Elmer) with a Pyris-Version 3.81 under nitrogen atmosphere. The sample weight was about 8 mg taken from the

middle of the samples. The temperature range was -10 to 250°C, the cycle consisted of first heating, cooling and second heating at 10 K/min.

Wide angle X-ray diffraction (WAXD) investigations were performed using a X-ray diffractometer P4C (Bruker axs) with monochromatized Cu-Kα radiation in a scattering range $2\Theta$ = 1.5 - 40° in transmission. Reflections at $2\Theta$ = 20.1° and 24.0° were assigned to the α-modification of PA6 crystals whereas, reflections at $2\Theta$ = 21.4° correspond to the γ-modification.[2]

## Results

### Blend Morphology

The selected blend composition is near the phase inversion composition of this blend system as shown by Kitayama for blends extruded under the same conditions[1]. Therefore, it was expected that variations in the extrusion conditions and the subsequent injection molding could change the morphology type.

Figure 1 shows micrographs of the blend extruded at 40 rpm obtained by different techniques.

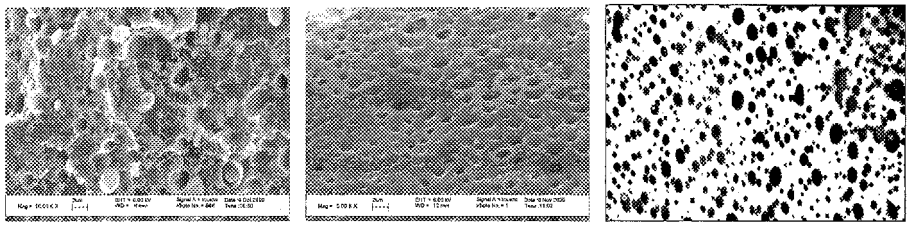

SEM, cryofracture | SEM, cryocut surface, etched with FA | TEM, PA6 stained (image size 34 x 24.5 µm)

Fig. 1. Morphology of PA6/SAN = 70/30 blend extruded at 40 rpm.

SEM cryofracture clearly indicates a matrix-disperse particle structure with nearly spherical particles. During cryofracture some of the dispersed particles dislodge from the matrix indicating poor phase adhesion between PA6 and SAN. SEM on etched surfaces and TEM show that PA6 is the dispersed phase. The particle size ranges between 0.2 and 2 µm.

After injection molding the morphology is changed significantly as shown in Figure 2.

The cryofractured surface also shows dispersed particles. TEM shows that the morphology is characterized by a particle in particle structure which is named in this paper as a "mixed structure". In the continuous phase of SAN small PA6 particles and islands of PA6 filled with small SAN droplets can be found. Etched surfaces also indicate that there are regions with SAN as the matrix component as well as regions with PA as the continuous phase. Such

structures typically are found for blend systems which experienced phase inversion during their mixing history.[3] The morphology of the blend extruded at 80 rpm is shown in Figure 3.

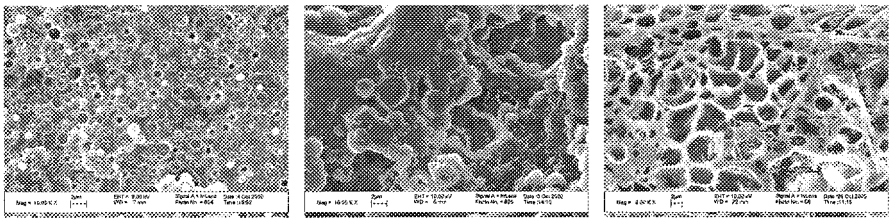

SEM, cryofracture SEM, cryocut surface, etched with FA etched with THF

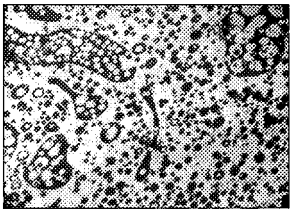

TEM, PA6 stained (image size 34 x 24.5 μm)

Fig. 2. Morphology of PA6/SAN = 70/30 blend extruded at 40 rpm and injection molded.

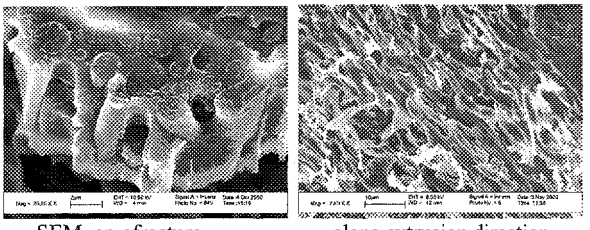

SEM, cryofracture along extrusion direction

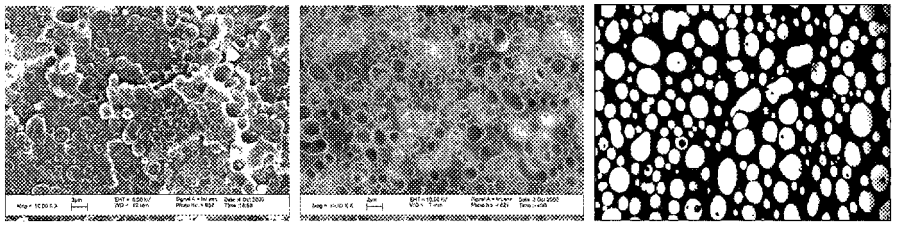

SEM, cryofracture SEM, cryocut surface, etched with THF TEM, PA6 stained (image size 34 x 24.5 μm)

Fig. 3. Morphology of PA6/SAN = 70/30 blend extruded at 80 rpm.

Fractures made along the extrusion direction clearly show that both materials form a co-continuous structure with elongated interconnected fibrils of both components in extrusion direction. SAN forms the convex surface part with PA6 filling the spaces between the SAN

strands. However, standard morphological investigations, as used for the blends mixed at 40 rpm, are not able to represent the co-continuous structure unequivocal. Investigating cryofractured surfaces or selectively etched cut surfaces oriented perpendicular to the extrusion direction could give the impression of particles of SAN in a PA6 matrix. Also TEM carried out on samples cut parallel to the extrusion direction could lead to the conclusion that PA6 forms the matrix phase with SAN particles in it. This result indicates the importance of carefully performed morphology investigations.

The morphological findings could be confirmed by solubility tests. Figure 4 shows vials with the blend materials dissolved in THF and formic acid, respectively. The strand extruded at 40 rpm clearly shows solubility in THF and insolubility in formic acid indicating SAN to be the matrix component. The injection molded 40 rpm sample shows partial solubility in both solvents in that there is a undissolved part in formic acid and THF indicating a "mixed structure" morphology. The strand extruded at 80 rpm retains its shape in both solvents indicating a continuous structure of both components. Quantitative analysis of the soluble parts showed a blend fraction soluble in formic acid of 29.8 wt% (PA6 content 30 wt%) and of 64.5 wt% soluble in THF (SAN content 70 wt%) confirming the existence of a co-continuous structure.

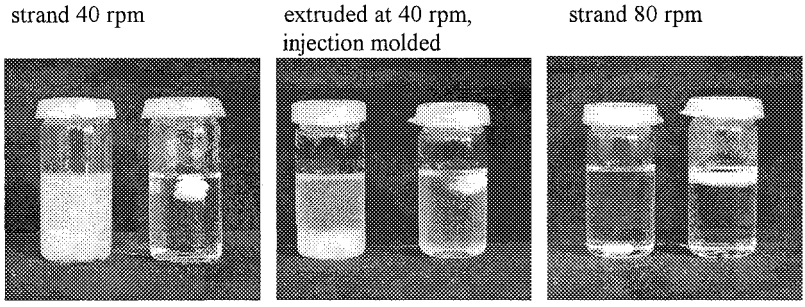


Fig. 4. Blends dissolved in THF (left vials) and formic acid (right vials).

**Melt Rheological Behavior of the Blends**

Melt rheological behavior is expected to show differences between the different types of morphology. Recently it was found by different authors that the elastic part of the complex viscosity, G', is very sensitive to the formation of co-continuity. Steinmann et al.[4] demonstrated that the value of G' at very low frequencies, representing the shape sensitive relaxation time range, is a suitable criterion for co-continuity. At the phase inversion composition, G' showed a significant maximum for all investigated PS/PMMA and SAN/PMMA blend systems having different viscosity ratios. This strong enhancement of the storage modulus was explained by extra stresses associated with the shape relaxation of the

interconnective structures. On the other hand, Galloway and Macosko[5] found maxima in G' at the onset compositions of co-continuity for PEO/PS blends exhibiting a broad co-continuous range. They explained these G' maxima with the interfacial area maxima at these compositions.[6] Prochazka et al.[7] confirmed these G' maxima for PEO/PVDF blends investigated at low frequencies (0.01 and 0.1 rad/s).

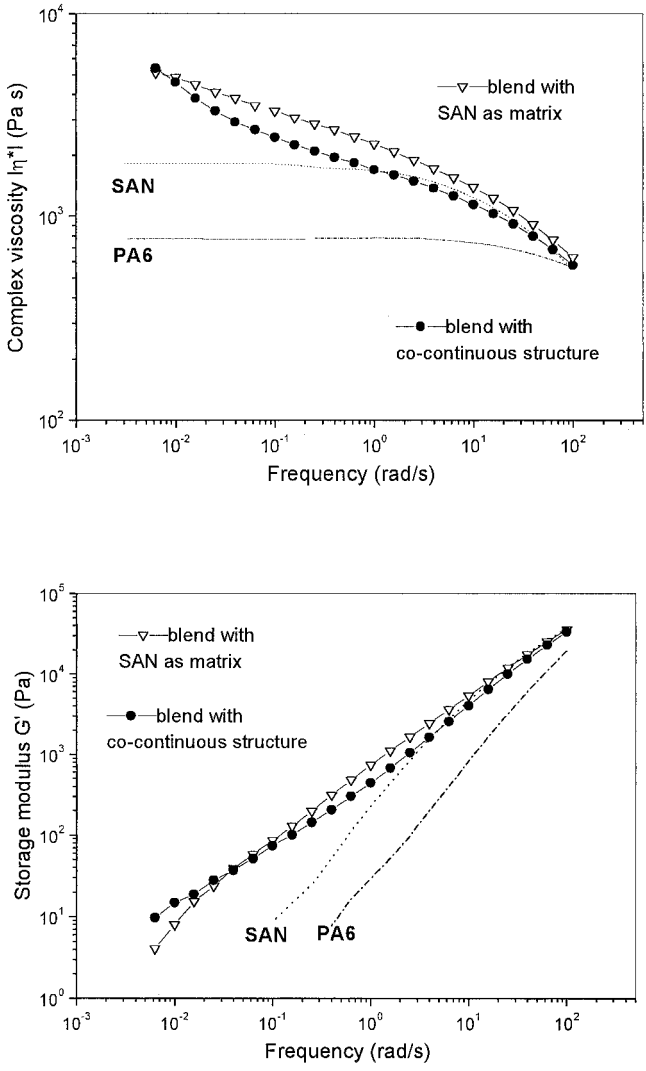


Fig. 5. Complex viscosity |η*| and storage modulus G' versus frequency for SAN/PA6 = 70/30 blends at 240°C.

Although all these considerations are made by changing the composition to switch from a dispersed to a co-continuous structure, we would like to determine if this criterion is also applicable to distinguish between a dispersed and a co-continuous structure having the same composition. Figure 5 shows the results of frequency sweeps performed at the mixing temperature.

At high frequencies, the blend based on the higher viscosity component as the continuous phase (SAN) and with PA6 as filler particles exhibits a higher blend viscosity than the co-continuous blend. In the co-continuous blend, both phases contribute more equally to the ultimate blend viscosity. However, the shapes of the viscosity versus frequency curves are different. At lower frequencies a significant increase in the blend viscosity of the co-continuos blend can be observed. This increase in viscosity seems to be characteristic for co-continuous blends and was also found by Steinmann et al.[4] by comparing dispersed and co-continuous PS/PMMA blends having different compositions. On the other hand, the G' behavior is complex. According to the higher G' value of SAN as compared to PA6 the blend based on SAN has a higher G' value at frequencies between 100 and 0.04 rad/s. Again the shape of the curve versus frequency is different from that of the co-continuous blend. By further decreasing the measurement frequency, G' becomes higher for the co-continuous blend than for the dispersed one. At 0.01 rad/s the dispersed blend exhibits a G' value of 7.9 Pa whereas the co-continuous one shows a G' value of 14.7 Pa. Even if the difference between the behavior of the co-continuous and the dispersed blend seems to be small, it was found to be characteristic and reproducible by measuring different samples. In addition, comparison of the first and third frequency sweep and the SEM micrographs before and after rheological measurements did indicate that there are no changes in the morphology type and structure size range caused by the rheological tests.

**Dynamic-Mechanical Analysis (DMA) of the Blends**

It is expected that co-continuous blends combine the moduli of the components in a much more effective way than dispersed blends where it is mostly dependent on the matrix behavior.[8,9] Gergen[10] presented an impressive example for SEBS/PC = 70/30 blends where in one case PC was the dispersed phase and in the other where co-continuous structure existed; for the co-continuous structure the storage modulus-temperature-dependency reflects a greater contribution of the rigid PC phase. Therefore, DMA should be a suitable method to distinguish between both structures.

Figure 6 shows the behavior of G' versus temperature.

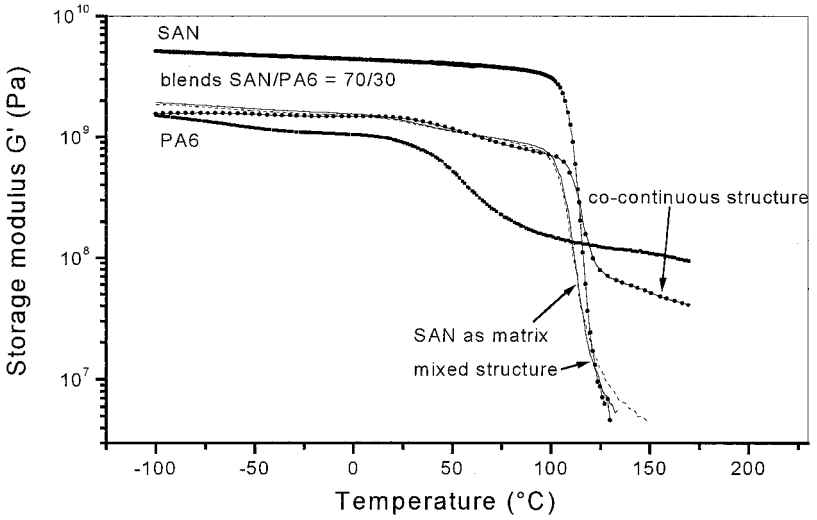


Fig. 6. Storage modulus G' versus temperature.

The differences between the G' values of the blends are only small in the temperature range up to the $T_g$ of SAN. The co-continuous structure shows slightly lower values than the other blends. Above the $T_g$ of PA6, the decrease in G' is slightly higher in the co-continuous blend but above the $T_g$ of SAN, significant differences become evident. The co-continuous blend exhibits much higher G' values than the other blends. Whereas, the dispersed blend and the blend with the mixed structure show a decrease in G' comparable to that of SAN; the blend with the co-continuous structure remains a much higher G' values in the range of that of PA6. The differences between the dispersed blend and the blend with the mixed structure are very small indicating that in the mixed structure, SAN is the main matrix component.

**Differential Scanning Calorimetry (DSC)**

The system contains an amorphous phase (SAN) and a crystallizable phase (PA6). It is known from the literature that when PA6 forms the disperse phase in blend systems, a "fractionated" crystallization behavior may be seen. This means that in the case of a lower crystallization or glass transition temperature of the matrix material, PA6 does not crystallize at temperatures typical for the bulk crystallization but it crystallizes with the matrix phase.[11] Fractionated crystallization was shown by Frensch et al.[11] for PVDF/PA6 blends and by Pompe et al.[12] for PP/PA6 blends. For the PP/PA6 system Pompe et al.[12] calculated the critical PA6 particle size

to be about 4 μm. Based on the particle sizes found in the blends under investigation here, fractionated crystallization behavior could be expected in the dispersed blend.

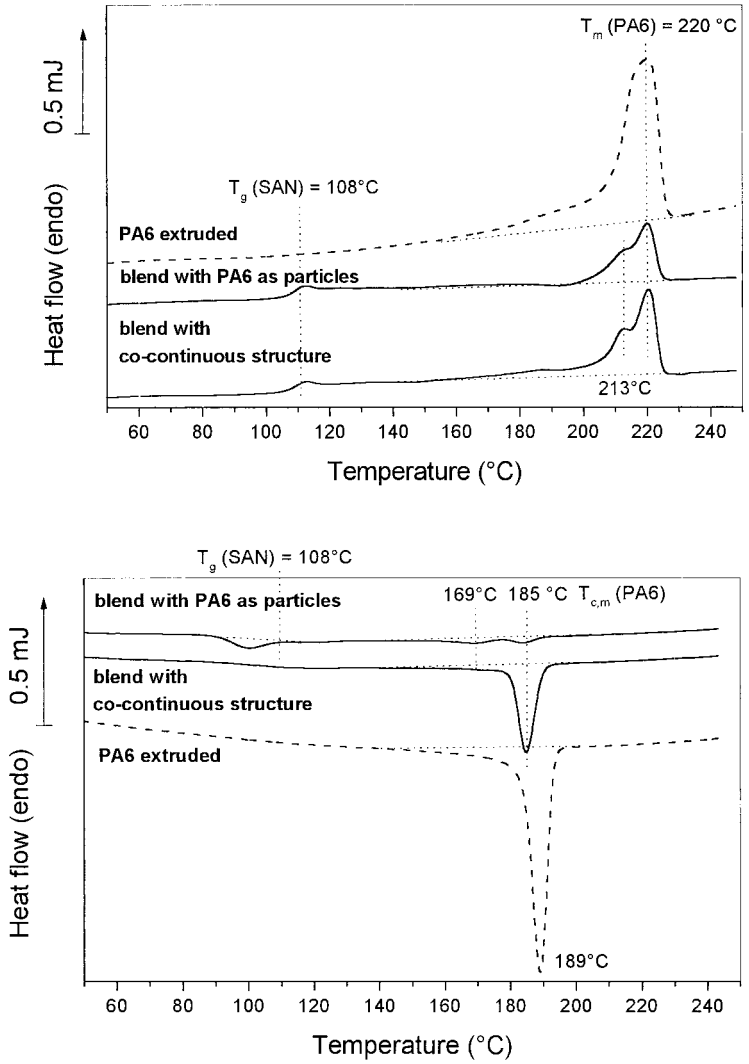


Fig. 7. Second heat (top) and cool (bottom) scans of SAN/PA6=70/30 blends and extruded PA6.

The results show that there really is a fractionated crystallization in the blend with SAN as matrix and PA6 as dispersed phase. In the co-continuous blend PA6 crystallizes in the temperature range typical for the extruded PA6; whereas, in the dispersed blend only a small

amount crystallizes at this temperature. Some of the PA6 phase appears to crystallize below the $T_g$ of the SAN phase. During the second heat, a cold crystallization at about 190°C is observed for the dispersed blend. However, the melting curves are very similar in both blends with a double peak (213°C and 220°C) indicating a transition from the $\gamma$ to the $\alpha$ crystal type of PA6 during heating (Figure 7). Additional WAXD investigations indicate that the unprocessed as well as the extruded PA6 exhibits only $\alpha$ crystallites whereas, all the blends only show $\gamma$ crystallites. Therefore, the differences in the crystallization behavior should not be due to different types of crystals. The crystallinity is clearly reduced in the dispersed blend which is evident by both DSC and WAXD results. Although different types of crystals are present in the PA6 component, the co-continuous blends exhibits about the same crystallinity as the processed PA6. Comparison of SEM micrographs on samples before and after DSC treatment did not show changes in the morphology type or phase size range.

## Summary and Conclusion

In a PA6/SAN blend near to its phase inversion composition it is possible to create different types of morphology by changing the melt blending conditions. Under the conditions selected, a screw speed of 40 rpm led to PA6 dispersed in SAN. Injection molding of the dispersed structure resulted in a "mixed structure" with SAN as main matrix and PA6 particles; whereas, some of the PA6 particles act as a matrix for SAN particles. Increasing the screw speed to 80 rpm produced a co-continuous morphology with an elongated orientation in the extrusion direction.

The co-continuous type of structure is especially difficult to identify by microscopic methods. Only the combination of different methods (SEM of cryofractures perpendicular and along the extrusion direction, SEM of selectively etched surfaces, and TEM) finally gives a clear picture of the morphology.

Solubility investigations confirmed the morphologies observed in the morphological investigations. This is a suitable and easy way to unequivocally detect co-continuous structures if one or both components have specific solvents.

Oscillatory melt rheological investigations show a clear difference between the dispersed and the co-continuous structure. At high frequencies, the blend based on the higher viscosity component as the continuous phase (SAN) and with PA6 as filler particles exhibits a higher melt viscosity than the co-continuous blend in which the viscosities of both components contribute more equally to the blend viscosity. However, in the low frequency range the co-

continuous blend shows similar $\eta^*$ and higher G' values than the dispersed one. It seems possible to deduce the type of morphology from the shape of the viscosity versus frequency and G' versus frequency curves when measured at low enough frequencies. A necessary condition (especially to get reliable values at low frequencies) is that the morphology has to be stable over the time frame of rheological investigation which was true for the blend system under investigation.

DMA indicated G' differences especially above the $T_g$ of SAN. Blends with SAN as matrix show a sharp decrease in G' whereas the co-continuous blend retains higher moduli due to the greater contribution from the higher modulus of PA6 in this temperature range. Therefore, DMA is also a suitable method to detect co-continuous structures when comparing the G' curves to that of the blend components.

DSC investigations could be used to distinguish between PA6 as dispersed phases and as part of a co-continuous structure. If PA6 forms the dispersed phase, its crystallization is prevented at the typical PA6 bulk crystallization temperature and a fractionated crystallization occurs. If PA6 forms a continuous phase as in a co-continuous structure, PA6 shows normal crystallization behavior. However, this method is limited to systems where phases are able to show a fractionated crystallization.

## Acknowledgement

The authors are grateful for the financial support granted by the Max-Kade-Foundation (New York) to P.P. during her stay at the University of Texas at Austin. We would like to thank Dr. Gisela Pompe (IPF Dresden) for assistance with the DSC measurements and result discussion and Dr. Dieter Jehnichen (IPF Dresden) for the WAXD measurements.

[1] N. Kitayama, H. Keskkula, D.R. Paul, *Polymer* **2000,** *41*, 8041.
[2] A. Galeski, A.S. Argon, R.E. Cohen, *Macromolecules* **1991,** *24*, 3945.
[3] C.W. Macosko, *Macrom. Symp.* **2000**, *149*,171.
[4] S. Steinmann, W. Gronski, Ch. Friedrich, *Rheol. Acta* **2002**, *41*, 77.
[5] J.A. Galloway, C.W. Macosko, *Conference Proceedings*, 3rd Pacific RIM Conference on Rheology, **2001**, July 08-13.
[6] J.A. Galloway, M.D. Montminy, C.W. Macosko, Polymer **2002**, *43*, 4715.
[7] F. Prochazka, C. Carrot, M. Castro, C. Celle, J.-C. Majesté, *Conference Proceedings,* PPS-18 Guimares Portugal, **2002**, June 16-20.
[8] L.A. Utracki, *Polymer Alloys and Blends: Thermodynamics and Rheology*; Hanser Publ.: München, **1989**, p. 178 ff.
[9] D.R Paul, S. Newman, *Polymer Blends, Volume 1*, Academic Press: New York, **1978**, 11-13.
[10] W.P. Gergen, R.G. Lutz, S. Davison, Hydrogenated Block Copolymers, Thermoplastic Elastomer Interpenetrating Polymer Networks. In: *Thermoplastic Elastomers*, 2nd ed.; G. Holden, N.R. Legge, R Quirk, H.E. Schroeder, Eds., Hanser Publ.: Munich, **1996,** 507.

[11] H. Frensch, H. Harnischfeger, B.-J. Jungnickel, Fractionated Crystallization in Incompatible Polymer Blends. In: *Multiphase Polymers: Blends and Ionomers,* L.A. Utracki, R.A. Weiss, Eds., ACS Symposium Series, **1989**, 101.
[12] G. Pompe, P. Pötschke, J. Pionteck, J. Appl. Polym. Sci. **2002,** *86,* 3445.